Universal multi-scale computations of Fourier integral operators for coherent imaging in caustics

Herwig Wendt and Maarten V. de Hoop, Purdue Univ.; Gunther Uhlmann, UC Irvine; Andràs Vasy, Stanford Univ.*

SUMMARY

Wave propagation, downward continuation, and imaging of seismic reflection data can be formulated in terms of a certain class of Fourier integral operators (FIOs). We present a procedure for the approximation and discretization of such operators following a multi-scale approach, viewing data through wave packets. Our algorithm is valid for the general class of FIOs associated with canonical graphs, allowing for anisotropy, and the formation of caustics. The key ingredient is the construction of a universal oscillatory integral representation via the introduction of singularity resolving diffeomorphisms, and the associated pseudo-differential partition of unity. As an example, we detail our approach for parametrices of evolution equations. We obtain a one-step algorithm for structured multi-scale wave-equation imaging and inverse scattering, time and depth extrapolation, velocity continuation, and extended imaging in general smoothly varying velocity models.

INTRODUCTION

Wave propagation, downward continuation and imaging can be formulated in terms of Fourier integral operators (FIOs) F associated with canonical graphs. In the absence of caustics, the action of F on a function u is given by *

$$(Fu)(y) = \int a(y,\xi)\exp(\mathrm{i}S(y,\xi))\hat{u}(\xi)\mathrm{d}\xi. \qquad (1)$$

The amplitude function $a(y,\xi)$ and the generating function $S(y,\xi) = P(y,\xi) - \langle \xi, y\rangle$ are determined by the ray geometry of the background medium. The latter describes the propagation of singularities according to de Hoop et al. (2009) $\chi : \left(\frac{\partial S}{\partial \xi}, \xi\right) \to \left(y, \frac{\partial S}{\partial y}\right)$. F has a sparse matrix representation with respect to the (co-)frame of "wave packets" (Smith (1998); Candès et al. (2006)). Where caustics occur, an extension needs to be constructed, in which locally (y,ξ) are standardly replaced by coordinate forms (y, x_I, ξ_J) (cf. (3) below). Here, we develop a universal algorithm for applying these FIOs using wave packets, allowing for anisotropy. To arrive at such an algorithm, we construct a universal oscillatory representation of their kernels using universal $(y,\tilde{\xi})$ coordinates, by introducing singularity resolving diffeomorphisms where caustics occur (cf. (4) below). The universal representation is of the form such that the "box-algorithm" recently developed by the authors, based on the dyadic parabolic decomposition of phase space, applies (Wendt et al. (2010)). This algorithm relies on the multi-scale expansion of low phase space separation rank of F in terms of geometric attributes, integrating wave packets and prolate spheroidal wave functions. Via its use, we arrive at an algorithm for the efficient discrete evaluation of the action of general operators in the universal representation we develop here, within accuracy $\mathcal{O}(2^{-k/2})$ at frequency scale 2^k. As an example of the FIO in the class considered here, we detail our construction and discrete approximation for solution operators F of evolution equations:

$$[\partial_t + \mathrm{i}P(t,x,D_x)]u = 0, \quad u|_{t=t_0} = u_0, \qquad (2)$$

on $X \subset \mathbb{R}^n$ and the interval $t \in [t_0, \mathscr{T}]$ with symbol P (in the case of the half wave equation, $P = P(x,\xi) = \sqrt{c(x)^2||\xi||^2}$). These operators generate extended imaging, include time and depth extrapolation (or downward continuation), wave-equation imaging and inverse scattering, and velocity continuation.

UNIVERSAL OPERATOR REPRESENTATION

Let $\varphi_\gamma(x)$, $\gamma = (j,\nu,k)$, denote a wave packet with central position $x_j^{\nu,k}$ and central wave vector $2^k\nu$, that is orientation ν at scale k. We consider Fourier integral operators, F, associated with canonical graphs. We allow the formation of caustics.

Fourier integral operators and caustics

Let (y, x_{I_i}, ξ_{J_i}) be local coordinates on the canonical relation, Λ say, of F, and S_i the corresponding generating function. Then $x_{J_i} = \frac{\partial S_i}{\partial \xi_{J_i}}$, $\xi_{I_i} = -\frac{\partial S_i}{\partial x_{I_i}}$, $\eta = \frac{\partial S_i}{\partial y}$. The coordinates are standardly defined on (overlapping) open sets O_i in Λ, $i = 1,\ldots,N$, where $(y, x_{I_i}, \xi_{J_i}) \to r(y, x_{I_i}, \xi_{J_i})$ is a diffeomorphism. We write $\sum_{i=1}^N \Gamma_i(r) = 1$, $r \in \Lambda$ for the corresponding partition of unity, and, in local coordinates, $\bar{\Gamma}_i(y, x_{I_i}, \xi_{J_i}) = \Gamma_i(r(y, x_{I_i}, \xi_{J_i}))$. Then $(F\varphi_\gamma)(y) = \sum_{i=1}^N (F_i\varphi_\gamma)(y)$ with

$$(F_i\varphi_\gamma)(y) = \int\int \bar{\Gamma}_i(y, x_{I_i}, \xi_{J_i}) a_i(y, x_{I_i}, \xi_{J_i}) \exp[\mathrm{i}(S_i(y, x_{I_i}, \xi_{J_i}) - \langle \xi_{J_i}, x_{J_i}\rangle]\ \varphi_\gamma(x)\mathrm{d}x\mathrm{d}\xi_{J_i}. \qquad (3)$$

The complex amplitude a_i accounts for the KMAH index. In the case of solution operators F of evolution equations, let p denote the principal symbol of P. Then, the bi-characteristics (rays) $(x,\xi) \to (y,\eta)$ of p define χ. The perturbations of (y,η) w.r.t. initial conditions (x,ξ) are collected in the propagator matrix $\Pi = \begin{pmatrix} W_1 & W_2 \\ W_3 & W_4 \end{pmatrix}$, and the rank-deficiencies of sub-blocks of Π determine the local coordinates in the vicinity of caustics: The sets I_i, J_i for admissible coordinate (y, x_{I_i}, ξ_{J_i}) are directly determined by the null space of the matrix W_1.

Singularity resolving diffeomorphism

We introduce local diffeomorphisms that enable us to express the operators F_i in terms of universal coordinates $(y,\tilde{\xi})$, and to apply the "box-algorithm" to (3). We begin with determining the rank of the matrix W_1 at the point $y_0 = y(x_0, \xi_0; \mathscr{T}, t_0)$ and $\xi = \xi_0$. If it does not have full rank here, we construct a diffeomorphism which removes the rank deficiency in a neighborhood of $r_0 = (y_0, \eta_0; x_0, \xi_0) \in \Lambda$. To be specific, we rotate coordinates, such that $\xi_0 = (1, 0, \ldots, 0)$ (upon normalization), and assume that the row associated with the coordinate x_2 gen-

*We denote by $\hat{\cdot}$ the Fourier transform of a function, and by ξ the Fourier (frequency) variables.

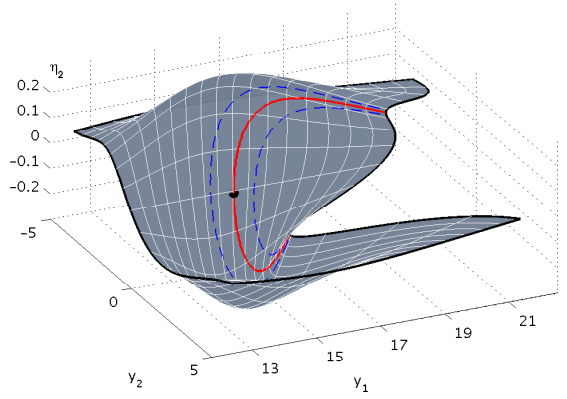

Figure 1: The canonical graph of F in our numerical example (ξ fixed), projected onto coordinates (y,η_2): caustic (red line), its vicinity (blue dashed line), and its tip (cusp) (black dot).

erates the rank deficiency (there could be more than one coordinate.) We then introduce the diffeomorphism,

$$Q : x \mapsto \tilde{x} = (x_1 - \frac{\alpha}{2}(x_2 - (x_0)_2)^2, x_2, \ldots, x_n); \qquad (4)$$

to preserve the symplectic form, we map $\xi \mapsto \tilde{\xi} = (\xi_1, \xi_2 + \alpha(x_2 - (x_0)_2)\,\xi_1, \xi_3, \ldots, \xi_n)$, yielding a canonical transformation C_Q : $(x,\xi) \mapsto (\tilde{x},\tilde{\xi})$. Q (and its inverse Q^{-1}) can be written in the form of an invertible Fourier integral operator with canonical relation given as the graph of C_Q (C_Q^{-1}, respectively). The corresponding propagator matrices Π_Q ($\Pi_{Q^{-1}}$) are obtained from their respective perturbations w.r.t. x ($\tilde{x}$). It follows that the composition $(\tilde{x},\tilde{\xi}) \overset{C_Q^{-1}}{\mapsto} (x,\xi) \overset{\chi}{\mapsto} (y,\eta)$ generates the graph of a canonical transformation, $\check{\chi}$ say, which can be parametrized by $(y,\tilde{\xi})$ locally on an open neighborhood of $(y_0,\tilde{\xi}(x_0,\xi_0))$. We compose F with Q^{-1} as Fourier integral operators: $\check{F} = FQ^{-1}$, with generating function $\check{S} = \check{S}(y,\tilde{\xi})$ and canonical relation the graph of $\check{\chi}$. The diagram in Fig. 2 illustrates the composition.

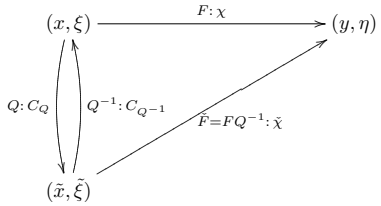

Figure 2: Relation between F, Q, Q^{-1} and $\check{F}$.

The composition operator $\check{F}$ is now formulated in universal coordinates $(y\tilde{\xi})$ and is caustic-free in the neighborhood of $(y_0,\eta_0;x_0,\xi_0)$ where F has a caustic. We illustrate this in Fig. 3 for a caustic generated by a low velocity lens.

Universal operator representation

For given types of rank deficiency (here, in x_2), we obtain a family of diffeomorphisms parametrized by (x_0,ξ_0). We only need a discrete set of diffeomorphisms $\{Q_{ij}\}_{j=1}^{N_i}$ to resolve the rank deficiencies leading to coordinates (y,x_{I_i},ξ_{J_i}) everywhere.

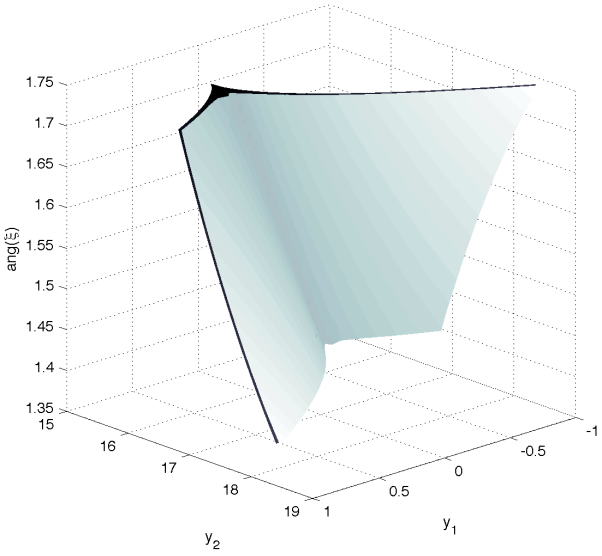

Figure 3: Caustic surfaces of F (dark grey) and $\check{F}$ (light grey) for a low velocity lens: The surfaces do not intersect.

We begin with subpartition $O_i = \cup_{j=1,\ldots,N_i} O_{ij}$ and construct the corresponding partition of unity $\sum_{i=1}^{N}\sum_{j=1}^{N_i}\Gamma_{ij}(r) = 1$ and operator factors as in (3). After inserting the diffeomorphisms, we have $\check{\Gamma}_{ij}(y,\tilde{\xi}) = \Gamma_{ij}(r(\tilde{r}(y,\tilde{\xi}))$, and we obtain $(F\varphi_\gamma)(y) = \sum_{i=1}^{N}\sum_{j=1}^{N_i}(F_{ij}\varphi_\gamma)(y)$ with operator factors

$$(F_{ij}\varphi_\gamma)(y) = \int \check{A}_{ij}(y,\tilde{\xi})\,\exp[\mathrm{i}\check{S}_{ij}(y,\tilde{\xi})]\,\widehat{Q_{ij}^*\varphi_\gamma}(\tilde{\xi})\,\mathrm{d}\tilde{\xi}, \qquad (5)$$

with universal coordinates $(y,\tilde{\xi})$ as in (1). Here, $\check{A}_{ij}(y,\tilde{\xi}) = \check{\Gamma}_{ij}(y,\tilde{\xi})\check{a}_{ij}(y,\tilde{\xi})$. To leading order, the amplitude $\check{a}_{ij}$ follows from the propagator matrix $\check{\Pi}_{ij} = \Pi\,\Pi_{Q_{ij}}^{-1}$.

UNIVERSAL FIO ALGORITHM

We develop a discrete approximate procedure for evaluating (5) for general input function u.

Partition of unity. We determine the sets O_i by monitoring the null space of the matrix W_1, and subpartition into sets on which the upper left sub-block of $\check{\Pi}_{ij}$ has full rank. Then we construct the corresponding partition functions $\check{\Gamma}_{ij}(y,\tilde{\xi})$ using double-exponential cutoffs of the form $\sim \exp(-\exp(d(y,\tilde{\xi}))$, where the function $d(y,\tilde{\xi})$ measures the distance from the boundary $\partial\check{O}_{ij}$. The partition of unity is formed by properly weighting the partition functions on the overlaps of the sets O_{ij}[†].

Diffeomorphism and re-decomposition. We begin with decomposing the data $u(x)$ into discrete almost symmetric wave packets (Duchkov et al. (2010)), enabling the fast evaluation of the Fourier transform of the data at sets of frequency points within the box $B_{\nu,k}$. From these, we obtain $Q^*\varphi_\gamma(\tilde{x})$ via evaluation of adjoint unequally spaced FFT (Dutt and Rokhlin (1993, 1995)) at points $x(\tilde{x})$. Then, we re-decompose into wave packets $\tilde{\varphi}_{\tilde{\gamma}}(\tilde{x})$ according to frequency boxes $B_{\tilde{\nu},k}(\tilde{\xi})$. We denote the data component corresponding to the box $B_{\tilde{\nu},k}$ by $\tilde{u}_{\tilde{\nu},k}(\tilde{x})$.

[†] In the following, we drop the subscript $_{ij}$.

Expansion of cutoff functions. The cutoff $\check{\Gamma}(y,\tilde{\xi})$ in (5) is homogeneous of degree zero in $\tilde{\xi}$ and is a classical smooth symbol (of order 0). We "subdivide" the integration over $\tilde{\xi}$, involving a (low-rank) separated representation of $\check{\Gamma}(y,\tilde{\xi})$ on the support of each relevant box in $\tilde{\xi}$ (Bao and Symes (1996); Beylkin et al. (2008)),

$$\check{\Gamma}(y,\tilde{\xi}) = \sum_{\beta=1}^{J_{\nu,k}} \check{\Gamma}_1^{\beta}(y)\check{\Gamma}_2^{\beta}(\tilde{\xi}), \quad \tilde{\xi} \in B_{\nu,k}. \tag{6}$$

One can view $\Gamma_2^{\beta}(\tilde{\xi})\hat{\chi}_{\nu,k}(\tilde{\xi})$ as a subdivision of the box $B_{\nu,k}$ into subsets (cones) of $\tilde{\xi}$. We know that $|J_{\nu,k}| \to 1$ as $k \to \infty$ since the cone of directions in $B_{\nu,k}$ shrinks as a function of $\sqrt{k}$. Hence, for large k this does not involve any action.

Application of "box-algorithm". We compute (5) with the box algorithm (Wendt et al. (2010); Andersson et al. (2011)), realizing the approximation to accuracy $\mathcal{O}(2^{-k/2})$ and discretization of the action of F on wave packets $\varphi_\gamma(x)$ in a common frequency box $B_{\nu,k}$. The approximation arises from the Taylor series expansion of $S(y,\xi)$ near the microlocal support of φ_γ. We illustrate its accuracy in Fig. 4. We obtain

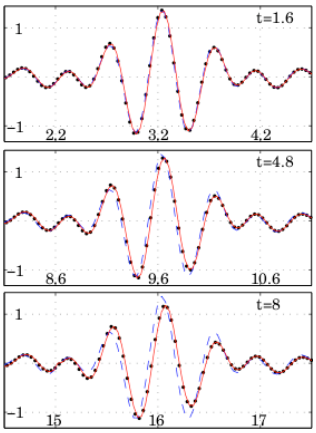

Figure 4: Evolution of a wave packet for (2) with $c(x) = c = 2km/s$ (central cross-sections): ray solution (blue dashed), finite difference (black dots), box-algorithm (red solid)

$$(F\varphi_\gamma)(y) \approx \sum_{\tilde{\nu}} \sum_{\beta=1}^{J_{\nu,k}} \check{\Gamma}_1^{\beta}(y)\check{a}(y,\tilde{\nu}) \sum_{r=1}^{R} \alpha_{\tilde{\nu},k}^{(r)}(y) \sum_{\xi\in B_{\tilde{\nu},k}} \check{\Gamma}_2^{\beta}(\tilde{\xi}) e^{\mathrm{i}\langle T_{\tilde{\nu},k}(y),\xi\rangle} \hat{\tilde{u}}_{\tilde{\nu},k}(\tilde{x}) |\hat{\tilde{\chi}}_{\nu,k}(\tilde{\xi})|^2 \hat{\vartheta}_{\tilde{\nu},k}^{(r)}(\tilde{\xi}). \tag{7}$$

Here, $T_{\tilde{\nu},k}(y)$ accounts for the propagation of singularities, and the expansion functions $\alpha_{\tilde{\nu},k}^{(r)}$ and $\hat{\vartheta}_{\tilde{\nu},k}^{(r)}$, obtained by coupling dyadic parabolic decomposition with prolate spheroidal wave functions Xiao et al. (2001), reproduce the second-order actions of $\check{F}$ (spreading, bending, dilation, shear, phase rotation along rays). We develop the expansion of $\check{S}$ relative to the central $\tilde{\xi}$ direction in the support of $\check{\Gamma}_2^{\beta}(\tilde{\xi})\hat{\tilde{\chi}}_{\nu,k}(\tilde{\xi})$. This reduces the number of expansion terms R and effectively balances the cost for the terms $J_{\nu,k}$ from the cutoffs. $\sum_{\tilde{\nu}}$ includes the boxes necessary for reproducing φ_γ under Q^{-1}. We can restrict to a small number of terms, while monitoring the energy loss and re-normalizing amplitudes. The computation of the first three sums in (7) is embarrassingly parallel.

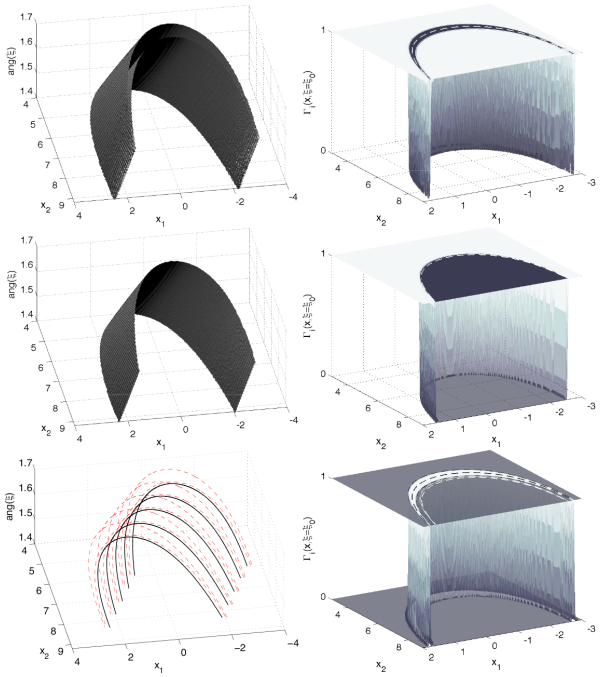

Figure 5: Iso-amplitude plots of $\Gamma_i(y,\xi)$ ($i = 1,3$, to left) $\Gamma_{21}(y,\xi)$ (center left), boundaries of the sets O_i (dashed) and O_{21} (solid) (left bottom). Right column: ξ-slices of cutoffs $\Gamma(y,\xi = \xi_0)$ for $i = 1,3$ (top), and for $ij = 21$ before (center) and after (bottom) weighting to form the partition of unity.

PARAMETRIX OF EVOLUTION EQUATION

We illustrate the principle of the universal operator representation and associated algorithm for propagation under the half wave equation. We choose a heterogeneous velocity model $c(x) = c_0 + \kappa\exp(-|x-x_0|^2/\sigma^2)$, containing a low velocity lens, with parameters $c_0 = 2km/s$, $\kappa = -0.4km/s$, $\sigma = 3km$, and $x_0 = (0,14)km$. As the initial data, we choose horizontal wave packets at frequency scale $k = 3$, respectively, in the vicinity of the point $x' = (0,5)km$. We fix the evolution time to $\mathscr{T} = 7s$. With this choice of parameters, most of the energy of the solution is concentrated near a cusp-type caustic.

We partition into three sets O_i, $i = \{1,2,3\}$. The sets $i = \{1,3\}$ are separated by the caustic. For these sets, we can choose coordinates (y,ξ), hence $Q_i = \mathbb{I}$. The set $i = 2$ contains the caustic. We plot these sets and the corresponding cutoff functions Γ_i in Fig. 5. For illustration purposes, in the factorization F_{ij} of F_i for $i = 2$, we choose to compute the operator $j = 1$, which resolves the singularity in an open neighborhood of the point indicated by a black dot on the canonical graph plotted in Fig. 1. This neighborhood contains the cusp of the caustic. We set $J_{\nu,k} = 1$ and restrict $\sum_{\tilde{\nu}}$ to 11 boxes neighboring the central orientation of the initial wave packet.

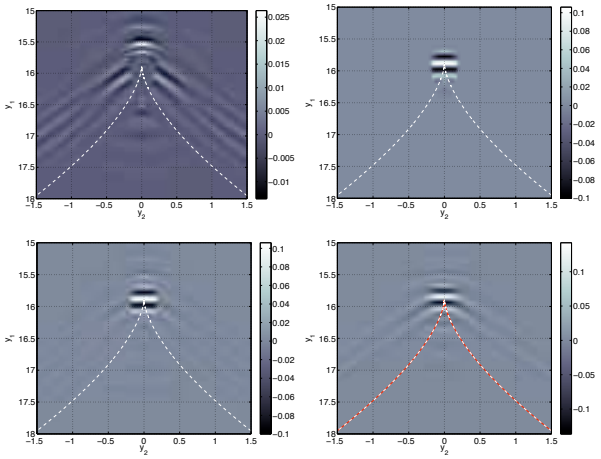

Figure 6: Action of $F \approx F_1 + F_3 + F_{21}$ in (5) on a single wave packet, evaluated using (7): $F_1 + F_3$ (top left), F_{21} (top right), $F_1 + F_3 + F_{21}$ (bottom left); finite difference computation (bottom right).

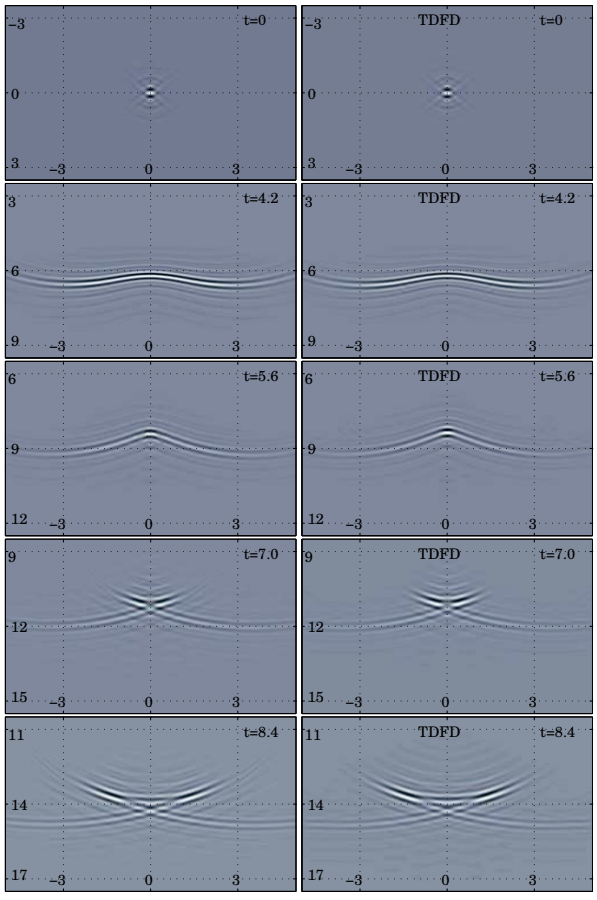

Figure 7: Multi-product computation of a wave front initiated by a band-limited delta-function through a caustic (left column): Initial data (top row), sequence of recompositions initializing the following operator in the multi-product (from row 2 to 4). Finite difference reference (right column).

In Fig. 6, we plot the different contributions obtained in our algorithm, and compare to a time domain finite difference computation (bottom right plot). The position of the caustic is indicated by the dashed line. We observe that our procedure has effectively removed the singularity. The phase of our computation matches the phase of the finite difference reference. This includes the KMAH index. For these initial data, most of the energy is contributed by F_{21} and concentrated in the vicinity of the open neighborhood in the vicinity of the tip of the cusp for which we have introduced the diffeomorphism Q_{21}. The amplitude produced by our algorithm is slightly weaker than the true amplitude, which reflects the fact that they have not been re-normalized in the re-decomposition step.

Multi-products of operators. For isotropic media, we can compute the action of F corresponding to the parametrix of an evolution equation for the interval $(t_0, \mathscr{T})$ as the action of a multi-product of operators, $F_{\mathscr{T},t_0} = F_{\mathscr{T},t_i} \circ F_{t_i,t_{i-1}} \circ \cdots \circ F_{t_1,t_0}$. Here, the partitioning t_i of the interval $(t_0, \mathscr{T})$ is chosen such that the operators $F_{t_i,t_{i-1}}$ are caustic-free, amounting to discretizing the evolution parameter into a sequence of (large) steps. Then, we can apply our algorithm for subsequently computing the action of the operators $F_{t_i,t_{i-1}}$ with diffeomorphisms Q set to identity. The computation of each operator in the multi-product is followed by a re-decomposition step, inducing a re-parametrization of the canonical relation that practically resolves the singularity, and initializing the following operator in the multi-product.

We illustrate this procedure in Fig. 7 for the above described velocity model. Here, the initial data consist of a delta-function, band-limited to a frequency cone with opening angle $\pm 40^\circ$, and to frequency scale $k = 3$. In the re-decomposition steps, we restrict to the subset of boxes at frequency scales $k = 2, 3, 4$ and with orientation $\pm 40^\circ$ about vertical, yielding the most significant contribution. We observe that our wave packet driven computation to accuracy $\mathscr{O}(2^{-k/2})$ reproduces the finite difference reference computation very well, despite the sequence of band-limiting re-decomposition steps involved.

CONCLUSIONS

We introduced a universal algorithm, based on wave packets as the quanta for representing seismic data, for imaging and inverse scattering of seismic reflection data. The algorithm allows for anisotropy and the formation of caustics. The method follows a multi-scale geometric approach and enables us to compress, de-noise and regularize the data, and to order and partition the information contained in them. As a key ingredient in the procedure, we have obtained a universal operator representation via the introduction of locally singularity diffeomorphisms. We can then apply an efficient and effective wave packet driven algorithm, integrating prolate spheroidal wave functions with the dyadic parabolic decomposition, which has been developed previously by the authors. Our modeling and imaging algorithm is valid for general dimension. This approach can be tied to a construction and iteration leading to the full wave solution in velocity models with limited smoothness (Andersson et al. (2008)).

REFERENCES

Andersson, F., M. de Hoop, and H. Wendt, 2011, Multi-scale discrete approximation of Fourier integral operators: SIAM MMS. (in revision).

Andersson, F., M. V. de Hoop, H. Smith, and G. Uhlmann, 2008, A multi-scale approach to hyperbolic evolution equations with limited smoothness: Comm. Partial Differential Equations, **33**, 988–1017.

Bao, G. and W. Symes, 1996, Computation of pseudo-dfferential operators: SIAM J. Sci. Comput., **17**, 416–429.

Beylkin, G., V. Cheruvu, and F. Pérez, 2008, Fast adaptive algorithms in the non-standard form for multidimensional problems: Appl. Comput. Harmon. Anal., **24**, 354–377.

Candès, E., L. Demanet, D. Donoho, and L. Ying, 2006, Fast discrete curvelet transforms: SIAM Multiscale Model. Simul., **5**, 861–899.

de Hoop, M., H. Smith, G. Uhlmann, and R. van der Hilst, 2009, Seismic imaging with the generalized radon transform: a curvelet transform perspective: Inverse Problems, **25**, 025005+.

Duchkov, A., F. Andersson, and M. de Hoop, 2010, Discrete almost symmetric wave packets and multi-scale representation of (seismic) waves: IEEE T. Geosci. Remote Sensing, accepted for publication.

Dutt, A. and V. Rokhlin, 1993, Fast Fourier transforms for nonequispaced data: SIAM J. Sci. Comput., **14**, 1368–1393.

———, 1995, Fast Fourier transforms for nonequispaced data II: Appl. Comput. Harmon. Anal., **2**, 85–100.

Smith, H., 1998, A parametrix construction for wave equations with $c^{1,1}$ coefficients: Ann. Inst. Fourier, Grenoble, **48**, 797–835.

Wendt, H., M. de Hoop, and F. Andersson, 2010, Multi-scale structured imaging using wave packets and prolate spheroidal wave functions: Presented at the Proc. SEG.

Xiao, H., V. Rokhlin, and N. Yarvin, 2001, Prolate spheroidal wave functions, quadrature and interpolation: Inverse problems, **17**, 805–838.